 MCB, vol.12, no.3, pp.215-230, 2015

Size-Dependent Diffusion of Dextrans in Excised Porcine Corneal Stroma

Ajith Rajapaksha[1,2], **Michael Fink**[1], **Brian A. Todd**[1]

Abstract: Delivery of therapeutic agents to the eye requires efficient transport through cellular and extracellular barriers. We evaluated the rate of diffusive transport in excised porcine corneal stroma using fluorescently labeled dextran molecules with hydrodynamic radii ranging from 1.3 to 34 nm. Fluorescence correlation spectroscopy (FCS) was used to measure diffusion coefficients of dextran molecules in the excised porcine corneal stroma. The preferential sensitivity of FCS to diffusion along two dimensions was used to differentially probe diffusion along the directions parallel to and perpendicular to the collagen lamellae of the corneal stroma. In order to develop an understanding of how size affects diffusion in cornea, diffusion coefficients in cornea were compared to diffusion coefficients measured in a simple buffer solution. Dextran molecules diffuse more slowly in cornea as compared to buffer solution. The reduction in diffusion coefficient is modest however (67% smaller), and is uniform over the range of sizes that we measured. This indicates that, for dextrans in the 1.3 to 34 nm range, the diffusion landscape of corneal stroma can be represented as a simple liquid with a viscosity approximately 1.5 times that of water. Diffusion coefficients measured parallel vs. perpendicular to the collagen lamellae were indistinguishable. This indicates that diffusion in the corneal stroma is not highly anisotropic. Our results support the notion that the corneal stroma is highly permeable and isotropic to transport of hydrophilic molecules and particles with hydrodynamic radii up to at least 34 nm.

Keywords: stroma, diffusion, nanoparticle, fluorescence correlation spectroscopy, confocal microscopy

1 Introduction

The most common and least invasive means for delivering drugs to the eye is to apply the drug topically and rely on its diffusion through the anterior layers of the

[1] Department of Physics and Astronomy, Purdue University, West Lafayette, IN 47907, USA
[2] Corresponding author E-mail: ajith@purdue.edu

eye. The tight cellular junctions of the corneal epithelium are often described as providing the greatest barrier to permeation, whereas, the corneal stroma is a thick but highly permeable layer [Dastjerdi, Sadrai, Saban, Zhang, and Dana (2011); Gaudana, Ananthula, Parenky, and Mitra (2010); Souto, Doktorovova, Gonzalez-Mira, Egea, and Garcia (2010); Yasueda, Higashiyama, Yamaguchi, Isowaki, and Ohtori (2007)]. This view is supported by diffusion measurements of molecules in the size range of 0.5-5 nm using permeation chambers and optical coherence tomography [Berezovsky, Patel, McCarey, and Edelhauser (2011); Ghosn, Tuchin, and Larin (2007); Gupta, Chauhan, Mutharasan, and Srinivas (2010); Prausnitz and Noonan (1998); Srirangam and Majumdar (2010); Urtti (2006); Wen, Trokel, Kim, and Paik (2013); Larin and Ghosn (2006)].

Many new and proposed therapeutics exploit sophisticated nanoparticle formulations [Souto, Doktorovova, Gonzalez-Mira, Egea, and Garcia (2010); Baba, Tanaka, Kubota, Kasai, Yokokura, Nakanishi, and Nishida (2011); Ribeiro, Sosnik, Chiappetta, Veiga, Concheiro, and Alvarez-Lorenzo (2012)] or biologics, such as, therapeutic proteins and nucleic acids [Brereton, Taylor, Farrall, Hocking, Thiel, Tea, and Williams (2005); Williams, Brereton, Farrall, Standfield, Taylor, Kirk, Coster (2005)]. Nanoparticles and macromolecules can be orders of magnitude larger than traditional small molecule drugs. Hence, it is important to determine whether the high permeability of the corneal stroma observed for small molecules will hold for nanoparticles and large macromolecules. A fiber matrix model for the corneal stroma based on structural considerations predicts that diffusion coefficients are strongly attenuated for molecular sizes greater than approximately 4 nm [Zhang, Prausnitz, and Edwards (2004); Edwards and Prausnitz (2001, 1998)]. However, there are yet no systematic experimental studies of size-dependent diffusion in the corneal stroma for molecular sizes above 5 nm.

Fluorescence correlation spectroscopy (FCS) measures diffusion coefficients by determining the average time required for fluorescent molecules to diffuse through a microscopic confocal illumination volume. FCS has been used extensively to characterize diffusion inside cells [Schwille et al. (1999)], in extracellular matrices [Masuda et al. (2005)], in mucus [Boukari et al. (2008)], and through bacterial biofilms [Briandet, Lacroix-Gueu, Renault, Lecart, Meylheuc, Bidnenko, Steenkeste, Bellon-Fontaine, and Fontaine-Aupart (2008); Guiot, Georges, Brun, Fontaine-Aupart, Bellon-Fontaine, and Briandet (2002)]. The confocal volume that probes diffusion in FCS is anisotropic, making FCS sensitive primarily to diffusion along the two directions perpendicular to the microscope optical axis. This can be used to characterize anisotropic diffusion by simply reorienting a sample with respect to the optical axis of the microscope [Gennerich and Schild (2002)].

We used FCS to measure tracer diffusion in porcine corneal stroma in the directions

parallel to the collagen lamellae and in the direction perpendicular to the collagen lamellae. We find that excised corneal stroma is highly permeable and isotropic for particles in the size range 1.3 to 34 nm. The dependence of the diffusion coefficient on the size of the diffusing species can be accounted for quantitatively using the simple Stokes-Einstein relationship that is used to describe diffusion through simple liquids. These results suggest that the diffusional landscape of the corneal stroma is more porous than previously thought. Consequently, we expect that the rapid permeation observed for small hydrophilic drugs through the corneal stroma can also be expected for hydrophilic nanoparticles and macromolecular therapeutics [Zhang, Prausnitz, and Edwards (2004); Edwards and Prausnitz (2001, 1998)].

2 Materials and Methods

2.1 Porcine Cornea and Sample Orientation

Porcine eyes were obtained from an abattoir as a byproduct of slaughter (Spear Products, Inc., Coopersburg Pennsylvania). Porcine cornea were chosen because the extant permeability data on porcine eyes closely match human eyes [Loch, Zakelj, Kristl, Nagel, Guthoff, Weitschies, and Seidlitz (2012)]. Cornea samples were obtained by excising a 0.5x0.5 cm patch from the center of the cornea. The epithelium layer was left intact. Excised cornea were incubated in Nunc Lab-Tek Chambered #1 Coverglass containing pH 7.4 phosphate buffered saline (hereafter referred to as "buffer") augmented with 5 nM of the fluorophore of interest at 4°C.

All measurements were made with the microscope objective directly in contact with the microscope coverglass. This maximizes the depth within the cornea at which diffusion is measured. In this configuration, the submicron sized confocal volume is focused to a depth past the epithelium and well into the corneal stroma. Consequently, our measurements reflect the properties of the corneal stroma only and are not affected by the presence of the epithelium.

Before adding the cornea to the chamber, we measured the intensity of fluorescence emission from the buffer/fluorophore solution. Upon adding cornea to the sample chamber we observed the fluorescence intensity dropped by a factor of 20, essentially reaching the background noise level. This guaranteed that the confocal observation was focused into the cornea and not in, for instance, into a solution filled gap between the cornea and the coverglass. For 2000 kD (the slowest diffusing molecule measured), the fluorescent intensity increased for a period of approximately 20 hours, finally stabilizing to a constant value. This indicates that the fluorophore reached its steady-state concentration within the corneal stroma for 2000 kD dextran solution within 20 hours. All other dextrans were smaller than 2000 kD and reached steady-state more rapidly. Diffusion coefficients were mea-

sured after a 20 hour incubation period and were monitored for time-dependent changes in diffusion coefficients. Each dextran was measured in cornea obtained from between 3 to 5 different eyes.

Measurements were made in two orientations relative to the optical axis, as shown in Fig. 1. FCS is primarily sensitive to diffusion along the two dimensions in the plane of the specimen, perpendicular to the optical axis. This allowed us to characterize diffusion parallel to the collagen lamella and diffusion perpendicular to the collagen lamella simply by reorienting the sample [Gennerich and Schild (2002)]. In the "para" orientation (Fig. 1(a)) the microscope optical axis is aligned with the anterior/posterior axis of the eye. In this orientation, the measurement is primarily sensitive to diffusion *parallel* to the collagen lamella of the corneal stroma. In the "trans" orientation (Fig. 1(c)), the microscope optical axis is aligned with the superior/inferior axis of the eye. Here, one of the two directions perpendicular to the microscope axis runs *transverse* to the collagen lamellae in the corneal stroma.

2.2 Fluorescently-labeled dextran

Fluorescently-labeled dextran were obtained in molecular weights ranging from 3kD to 2000kD. The following tetramethylrhodamine-labeled dextrans were obtained from Invitrogen Life Technologies (Carlsbad, CA): 3kD dextran (#: D3307), 10kD dextran (#: D1816), 40kD dextran (#: D1942) and 2000kD Dextran (#: D7139). Rhodamine-labeled 500kD Dextran (#: DX500-RB-1) was purchased from Nanocs Inc. (Boston, MA). Tetramethylrhodamine-isothiocyanate dextran of molecular weight 155kD (#: T1287) was purchased from Sigma-Aldrich (St. Louis, MO). All dextrans were used without further purification.

2.3 Fluorescence Correlation Spectroscopy (FCS)

FCS was performed with an ISS Alba (Champaign, IL) using a 532 nm Coherent Compass 115M-5 laser (Santa Clara, CA) and a Olympus DPlan 100X, 1.25 NA oil immersion objective. The confocal pinhole was implemented using the 50 μm aperture on the Micron Photon Devices PDM Series avalanche photodiodes (San Jose, CA). The dimensions of the focal volume were calibrated by measuring the diffusion of Alexa532 (Invitrogen, Product#: A20001) at 2.5, 5, and 10 nM concentrations and fitting a single species correlation function to find the major and minor dimensions of the elliptical focal volume. The value of the Alexa532 diffusion coefficient used for the calibration was 398 μm^2/s [Nitsche, Chang, Weber, and Nicholson (2004); Petrasek and Schwille (2008)]. Typical calibrated focal volume dimensions were 0.3 μm in the direction perpendicular to the optical axis and 9 μm in the direction along the optical axis. We expect that this observation volume is sufficiently small that it will characterize specifically the stroma of the cornea but

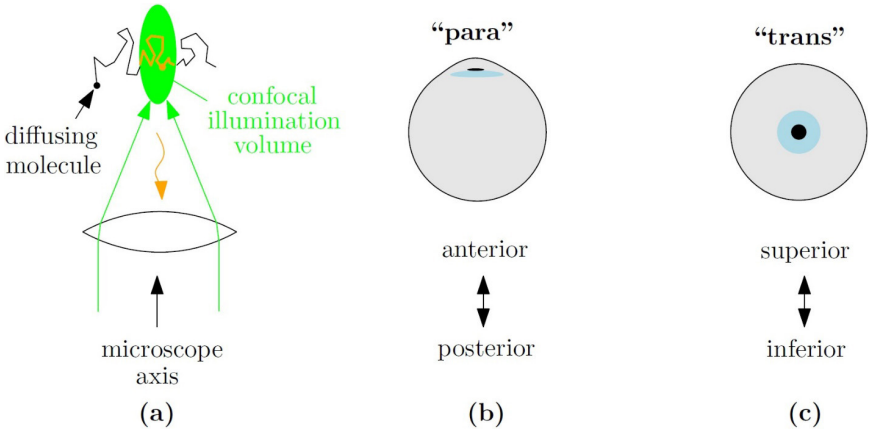

Figure 1: Experimental Schematic and Sample Geometry. (a) Fluorescence correlation spectroscopy (FCS) measures diffusion coefficients from the time-dependent fluctuations in fluorescence intensity measured using a confocal microscope. Fluctuations in fluorescence intensity are caused by fluorescent molecules diffusing through the illumination volume (shown in green) and emitting fluorescence (shown in orange) for a period of time that is characteristic of the molecule's diffusion coefficient. The focal volume has an elliptical shape and measurements are primarily sensitive to diffusion along the two shorter dimensions of the ellipse, i.e. perpendicular to the microscope optical axis (indicated by black arrow). We used this to measure diffusion coefficients in the corneal stroma in two different orientations. (b) In the "para" orientation, the microscope axis is aligned with the anterior/posterior axis of the eye and the measurement is primarily sensitive to diffusion *parallel* to the collagen lamella in the corneal stroma. (c) In the "trans" orientation, the microscope axis is aligned with the superior/inferior axis of the eye and one of the two directions perpendicular to the microscope axis runs transverse to the collagen lamellae in the corneal stroma.

sufficiently large that it will sample over many collagen lamellae.

For each fluorophore, we measured the FCS signal with decreasing laser excitations until we observed that the measured diffusion coefficient did not depend on the excitation intensity. This guaranteed the absence of photo-bleaching artifacts. Emitted fluorescence was split using a 50:50 beam splitter and recorded on two separate avalanche photodiodes. These were cross-correlated to avoid the detector after-pulsing artifact that arises when auto-correlating the fluorescence fluctuations from a single detector. Cross-correlation functions for dextran could not be fit to single species model because of poly-dispersity in the dextran molecules. In order to determine the diffusion coefficient of dextrans, we determined the value of the

time lag, τ_{50} where the normalized cross-correlation time dropped by ½ its value at zero time lag. The diffusion coefficient was then given by comparison to the Alexa532 calibration standard,

$$D_{Dextran} = D_{Alexa532} \frac{\tau_{50,Alexa532}}{\tau_{50,Dextran}}. \quad (1)$$

2.4 Modeling diffusion

The size-dependence for diffusion of macromolecules in homogeneous liquids (e.g. water or buffer) can be described by the Stokes-Einstein Eq. [Atkins (1994)],

$$D = \frac{k_b T}{6\pi\eta R} \quad (2)$$

where D is the diffusion coefficient, k_b is Boltzmann's constant, T is temperature, η is viscosity, and R is the hydrodynamic radius of the diffusing species. For water or buffer at 25°C, $\eta \sim 0.91\text{x}10^{-3}$ Pa.s and $k_b T \sim 4.1\text{x}10^{-21}$ J. In order to determine the hydrodynamic radii for our dextran molecules, we measured diffusion coefficients in buffer by FCS and used Eq. 2 to calculate the hydrodynamic radii, R. Our measured values of R were within 20% of those previously measured for similar molecular weights [Armstrong, Wenby, Meiselman, and Fisher (2004); Braga, Desterro, and Carmo-Fonseca (2004); Bu and Russo (1994); Fahner et al. (1984); Gregor, Bialek, van Steveninck, Tank, and Wieschaus (2005); Lawrence, Wolfaardt, and Korber (1994); Yuan, Lv, Zeng, and Fu (2009); Zhang, Nadezhina, and Wilkinson (2011)].

In order to characterize the size-dependence for diffusion in cornea we plot the measured diffusion coefficients for dextrans in cornea versus the dextran hydrodynamics radii determined in buffer. Because of the large range of diffusion coefficients and hydrodynamic radii, we plot both axis on a logarithmic scale. For the simple relationship predicted by Eq. 2 this gives,

$$\log D = \log \frac{k_b T}{6\pi\eta} - \log R. \quad (3)$$

From this equation it can be seen that the hallmark for diffusion, obeying the Stokes-Einstein Equation, is that a plot of $\log D$ vs. $\log R$ has a slope of -1. In many biological samples where large molecules are hindered by nanoscopic obstacles (e.g. the cytoskeleton for diffusion inside cells), the dependence of diffusion coefficient on size is stronger than predicted by the Stokes-Einstein [Dix and Verkman (2008)]. On a plot of $\log D$ vs. $\log R$ this stronger dependence would be manifest by a slope decreasing more steeply than -1.

2.5 Statistical Analysis

In order to calculate statistical uncertainty, we pooled all measurements for a single cornea and single dextran molecular weight into one mean value. We consider that this mean contributes one independent measurement. All error bars represent standard errors of the mean where the number of measurements is the number of different cornea. *P*-values were calculated using independent two group t-tests. All statistical tests were performed using "t.test" in the *R* statistical computing environment Version 3.0.3.

3 Results

Figure 2 shows the raw FCS data for an Alexa532 calibration standard measured in buffer (green line), a 2000 kD rhodamine-labeled dextran in buffer (black line), and for a 2000 kD rhodamine-labeled dextran in cornea in the para orientation (red line). The important parameter obtained from each curve is τ_{50}, the value of the time lag at which the normalized correlations drop below ½. Roughly speaking, this number represents the average residence time that a diffusing particle spends in the focal volume. Rapid diffusion corresponds to small τ_{50}, whereas, slow diffusion corresponds to large τ_{50}. For Alexa532 (green curve), the τ_{50} of approximately 10^{-4} s is indicated on the Figure.

2000 kD dextran is a much larger molecule than Alexa532 and, consequently diffuses much more slowly. This is reflected in the fact that the curve for 2000 kD dextran in buffer is shifted to the right relative to Alexa532 (black curve is shifted to the right relative to green curve). The cross-correlation function measured for 2000 kD dextran in cornea shifts yet further to the right, as compared to 2000 kD dextran in buffer (red curve is shifted to the right relative to black curve). This indicates that the diffusion coefficient for 2000 kD dextran is smaller in cornea, as compared to the diffusion coefficient in buffer. Diffusion coefficients for all dextrans were calculated from τ_{50} values using data analogous to that shown in Fig. 2, along with Eq. 1.

We sought to determine whether the diffusion coefficients changed over the incubation period by comparing diffusion coefficients measured at 1, 2, and 3 days post-incubation (Fig. 3). Between day 1 and 3, the average change in diffusion coefficient was -12% with a standard deviation of 30%. The *p*-value was 0.19 against the null hypothesis that the diffusion coefficients did not change. Consequently, we conclude that changes in the diffusion coefficient over the 3 day measurement period were not significant. For all subsequent analysis, measurements were combined over the entire observation period. Mean values and standard errors of the mean for the combined data are given in Table 1.

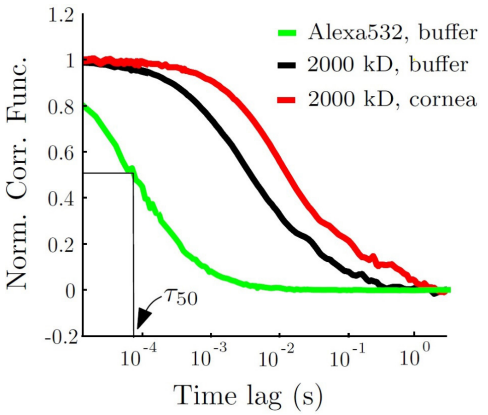

Figure 2: Fluorescence correlation spectroscopy (FCS) data for Alexa532 in buffer (green), rhodamine-labeled 2000 kD dextran in buffer (black), and 2000 kD dextran in corneal stroma (red). Diffusion coefficients are measured by determining the duration over which fluorescence emission from the confocal volume are correlated in time; the slower the diffusion, the greater the time over which a fluorescence signal will be correlated. 2000 kD dextran is a large molecule and diffuses in buffer more slowly than the smaller Alexa532 (black is shifted to right relative to green). When 2000 kD dextran is measured in cornea, the normalized correlation function shifts to the right relative to 2000 kD dextran in buffer solution (red shifted to the right relative to black). This indicates that diffusion in cornea is slower than in buffer.

Figure 4 compares diffusion coefficients measured for all dextrans in buffer (black) as compared to diffusion coefficients measured for dextrans in corneal stroma in the para orientation (red). Error bars represent the standard error of the mean. All diffusion coefficients measured in cornea were significantly less than those measured in buffer; p-values range from $3\text{x}10^{-6}$ to $3\text{x}10^{-2}$ against the null hypothesis that the means in cornea are the same as those in buffer. When plotted, as in Fig. 3, on a log scale, the relationship between diffusion coefficients and hydrodynamic radii in cornea can be obtained by simply shifting downward each diffusion coefficient by 67%, relative to its value in buffer. That the slope of $\log D$ vs. $\log R$ remains -1 in cornea indicates that the relationship between diffusion coefficient and hydrodynamics radius in cornea can be described by the Stokes-Einstein equation, Eq. 2. The 67% decrease in diffusion coefficients in going from buffer to cornea can be accounted for by a viscosity for corneal stroma that is 1.5 times as large as the viscosity of the buffer (red line in Fig. 4 with Eq. 3 and viscosity 1.5 times that in water).

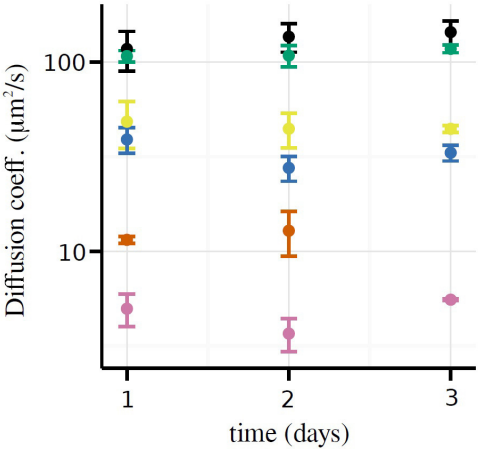

Figure 3: Diffusion coefficients in corneal stroma as a function of time, post-incubation. Symbols indicate mean values and error bars are standard errors of the mean for dextrans of molecular weight: 3 kD (black), 10 kD (green), 40 kD (yellow), 155 kD (blue), 500 kDa (orange), 2000 kD (purple).

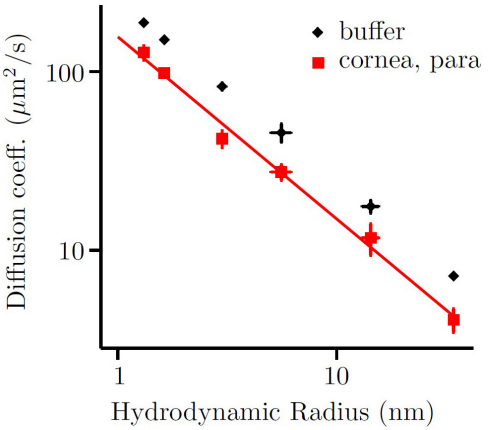

Figure 4: Size-dependent diffusion of dextran in buffer solution (black) and in cornea in the para orientation (red). Symbols indicate mean values and error bars are standard errors of the mean. All average diffusion coefficients measured in cornea are significantly smaller than those measured in buffer ($p < 3\text{x}10^{-2}$). The decrease in diffusion coefficient in moving from buffer to cornea can be accounted for by an increase in the viscosity of cornea by 1.5 times that of buffer (Eq. 3, red line).

Table 1: Mean diffusion coefficients for dextrans measured in buffer, corneal stroma in the para orientation, and corneal stroma in the trans orientation. "±" indicates the standard error of the mean with the number of different cornea ranging from 3 to 5.

MW (kDa)	R_h (nm)	D_{buffer} (μm^2/s)	$D_{stroma,para}$ (μm^2/s)	$D_{stroma,trans}$ (μm^2/s)
5	1.31 ± 0.04	187 ± 5	123 ± 12	-
10	1.63 ± 0.03	151 ± 3	98 ± 4	-
40	3.0 ± 0.1	83 ± 3	42 ± 6	60 ± 9
155	5.6 ± 0.6	46 ± 5	27 ± 3	28 ± 8
500	14 ± 1	18 ± 2	12 ± 2	8 ± 2
2000	34 ± 1	7.2 ± 0.2	4 ± 0.6	4 ± 1

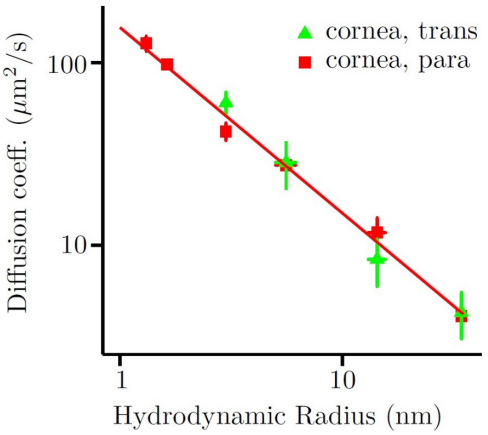

Figure 5: Size-dependent diffusion of dextran in para orientation (red) vs. trans orientation (green). Symbols indicate mean values and error bars are standard errors of the mean. We do not detect any significant differences between diffusion in the two orientations ($p > 0.12$), indicating that diffusion in the corneal stroma is isotropic.

Figure 5 compares diffusion coefficients measured in the "para" orientation with the same measurements made in the "trans" orientation (see Fig. 1 for definition of these two orientations). There are no systematic differences between the two sets of measurements; p-values range from 0.12 to 0.92 against the null hypothesis that the mean in the para orientation is the same as the mean in the trans orientation. This indicates that, despite considerable anisotropy in the collagen lamellae of cornea, diffusion is not highly anisotropic.

4 Discussion

Size is an important factor in the penetration of therapeutics through biological tissues. Size-dependent diffusion, inside cells [Schwille et al. (1999)], in extracellular matrices [Masuda et al. (2005)], in mucus [Boukari et al. (2008)], and through bacterial biofilms [Briandet, Lacroix-Gueu, Renault, Lecart, Meylheuc, Bidnenko, Steenkeste, Bellon-Fontaine, and Fontaine-Aupart (2008); Guiot, Georges, Brun, Fontaine-Aupart, Bellon-Fontaine, and Briandet (2002)] have been characterized experimentally and a wide range of behaviors have been observed. For instance, many intracellular environments exhibit a sieving property where small molecules diffuse freely but transport of objects larger than 10-30 nm is severely restricted [Dix and Verkman (2008)]. Other biological materials, such as mucus, are highly porous even for particles as large as 100 nm [Lai, Wang, Hida, Cone, and Hanes (2010)]. A fiber matrix model for the corneal stroma predicts that diffusion in cornea will be strongly attenuated for objects larger than approximately 4 nm [Zhang, Prausnitz, and Edwards (2004); Edwards and Prausnitz (2001, 1998)]. Ours is the first study to systematically study the size dependence of diffusion in corneal stroma for objects with hydrodynamic radii greater than 5 nm.

We measured size-dependent diffusion in excised porcine corneal stroma for dextran polymers with hydrodynamic radii between 1.3 and 34 nm. We expected larger polymers to experience a hindrance from the collagen fibrils that would depend on cornea orientation. In contrast to our expectations, we found that all dextrans, regardless of size, exhibited diffusion coefficients that were around 67% as large as their values in buffer. No size-dependence beyond what is predicted by the Stokes-Einstein relationship (Eq. 2) was observed. This indicates that, at least up to a particle radius of 34 nm, the collagen meshwork of excised porcine corneal stroma does not ensnare diffusing particles. Measurements of diffusion along the directions parallel and perpendicular to the collagen lamella were indistinguishable, indicating that diffusion in excised cornea is not highly anisotropic. Taken together, our results suggest that excised cornea is permeable for objects up to 34 nm in hydrodynamic radii and that the size-dependence for diffusion through excised porcine cornea can be described simply by the Stokes-Einstein Eq. with a viscosity approximately 1.5 times that of buffer (red line in Fig. 4).

A major limitation of our study is that, similar to most previous studies on corneal stroma diffusion (i.e. 4 of the 5 studies reviewed by Prausnitz and Noonan (1998)), our experiments utilized excised cornea. Under these conditions, the ultrastructure of the stroma involving a precise arrangement of collagen fibrils as well as their lamellae could be lost. Stroma can swell substantially when exposed to water and this could cause the lamellar collagen structure to be more expanded in excised cornea, as compared to cornea *in vivo.* This may account for the absence of strong

size dependence in our experimental data. Because our measurements reflect excised cornea stroma, the absolute dextran diffusion coefficients observed in our studies should be applied to *in vivo* models only with caution. Our findings can be directly applied to cornea used for transplantation which are excised and stored for up to 10 days [Pels, Beele, and Claerhout (2008)].

Our results can be compared to the extent data on diffusion within the stroma, the majority of which reflect excised cornea [Prausnitz and Noonan (1998)]. These previous measurements show that diffusion coefficients for small hydrophilic molecules in cornea tend to be $\sim 50\%$ as large as their values in water or buffer [Prausnitz and Noonan (1998)]. Given that boundary effects in permeation chamber studies tend to lead to under-estimation of diffusion coefficients [Sanders, De Smedt, and Demeester (2000)], we consider these measurements to be similar to our findings that diffusion coefficients in cornea are 67% as large as those in buffer. It was predicted that the high permeabilities observed for small molecules would not extend to molecules larger than approximately 4 nm [Zhang, Prausnitz, and Edwards (2004); Edwards and Prausnitz (2001, 1998)]. However, this is the first systematic experimental studies of size-dependent diffusion in the corneal stroma for molecular sizes above 5 nm. Contrary to expectations, we find that the corneal stroma is permeable for objects up to sizes of at least 34 nm. Transmission electron microscopy studies performed on human cornea report that the collagen fibrils in corneal stroma have inter-fibril spacing of 20 to 50 nm [Komai and Ushiki (1991); Sanchez, Martin, Ussa, and Fernandez-Bueno (2011). We observed relatively unattenuated diffusion in corneal stroma for dextran with hydrodynamic radii ranging from 1.3 to $34\sim$nm. Given that our dextran hydrodynamic radii are smaller or comparable to interfibril spacing observed in structural studies of cornea, we consider that our diffusion measurements are consistent with these structural studies.

An additional limitation of our study was that we characterized diffusion purely within the corneal stroma. Permeation into the eye requires, additionally, permeation through the corneal epithelium and through additional anterior layers of the eye. Our work demonstrates that FCS, which probes a microscopic region of space, could be a useful technique for independently characterizing the various compartments of the eye. This, in turn, can be used to parameterize and validate sophisticated pharmokinetic models for drug delivery to the eye.

Acknowledgement: The research was support by National Science Foundation (1006485-DMR). We thank Michael Fink (M.S.) for his contributions to the work by establishing Alexa532 calibration standards for the FCS system.

References

Dastjerdi, M. H.; Sadrai, Z.; Saban, D. R.; Zhang, Q.; Dana, R. (2011): Corneal penetration of topical and subconjunctival bevacizumab. *Investigative Ophthalmology & Visual Science,* vol. 52, pp. 8718–8723.

Gaudana, R.; Ananthula, H. K.; Parenky, A.; Mitra, A. K. (2010): Ocular drug delivery. *AAPS Journal,* vol. 12, pp. 348–360.

Souto, E. B.; Doktorovova, S.; Gonzalez-Mira, E.; Egea, M. A.; Garcia, M. L. (2010): Feasibility of lipid nanoparticles for ocular delivery of anti-inflammatory drugs. *Current Eye Research,* vol. 35, pp. 537–552.

Yasueda, S.; Higashiyama, M.; Yamaguchi, M.; Isowaki, A.; Ohtori, A. (2007): Corneal critical barrier against the penetration of dexamethasone and lomefloxacin hydrochloride: Evaluation by the activation energy for drug partition and diffusion in cornea. *Drug Development and Industrial Pharmacy,* vol. 33, pp. 805–811.

Berezovsky, D. E.; Patel, S. R.; McCarey, B. E.; Edelhauser, H. F. (2011): In vivo ocular fluorophotometry: delivery of fluoresceinated dextrans via transscleral diffusion in rabbits. *Investigative Ophthalmology & Visual Science,* vol. 52, pp. 7038–7045.

Ghosn, M. G.; Tuchin, V. V.; Larin, K. V. (2007): Nondestructive quantification of analyte diffusion in cornea and sclera using optical coherence tomography. *Investigative Ophthalmology & Visual Science,* vol. 48, pp. 2726–2733.

Gupta, C.; Chauhan, A.; Mutharasan, R.; Srinivas, S. P. (2010): Measurement and modeling of diffusion kinetics of a lipophilic molecule across rabbit cornea. *Pharmaceutical Research,* vol. 27, pp. 699–711.

Prausnitz, M. R.; Noonan, J. S. (1998): Permeability of cornea, sclera, and conjunctiva: A literature analysis for drug delivery to the eye. *Journal of Pharmaceutical Sciences,* vol. 87, pp. 1479–1488.

Srirangam, R.; Majumdar, S. (2010): Passive asymmetric transport of hesperetin across isolated rabbit cornea. *International Journal of Pharmaceutics,* vol. 394, pp. 60–67.

Urtti A. (2006): Challenges and obstacles of ocular pharmacokinetics and drug delivery. *Advanced Drug Delivery Reviews,* vol. 58, pp. 1131–1135.

Wen, Q.; Trokel, S. L.; Kim, M.; Paik, D. C. (2013): Aliphatic beta-nitroalcohols for therapeutic corneoscleral cross-linking: corneal permeability considerations. *Cornea,* vol. 32, pp. 179–184.

Larin, K. V.; Ghosn, M. G. (2006): Optical coherent tomography measurements of the diffusion rate of water and drugs in an isolated and whole cornea. *Quantum Electronics,* vol. 36, pp. 1083–1088.

Baba, K.; Tanaka, Y.; Kubota, A.; Kasai, H.; Yokokura, S.; Nakanishi, H.; Nishida, K. (2011): A method for enhancing the ocular penetration of eye drops using nanoparticles of hydrolyzable dye. *Journal of Controlled Release,* vol. 153, pp. 278–287.

Ribeiro, A.; Sosnik, A.; Chiappetta, D. A.; Veiga, F.; Concheiro, A.; Alvarez-Lorenzo, C. (2012): Single and mixed poloxamine micelles as nanocarriers for solubilization and sustained release of ethoxzolamide for topical glaucoma therapy. *Journal of the Royal Society Interface,* vol. 9, pp. 2059–2069.

Brereton, H. M.; Taylor, S. D.; Farrall, A.; Hocking, D.; Thiel, M. A.; Tea, M.; Williams, K. A. (2005): Influence of format on in vitro penetration of antibody fragments through porcine cornea. *British Journal of Ophthalmology,* Vols. 1205–1209, p. 89.

Williams, K. A.; Brereton, H. M.; Farrall, A.; Standfield, S. D.; Taylor, S. D.; Kirk, L. A.; Coster, D. J. (2005): Topically applied antibody fragments penetrate into the back of the rabbit eye. *Eye,* vol. 19, pp. 910–913.

Zhang, W.; Prausnitz, M. R.; Edwards, A. (2004): Model of transient drug diffusion across cornea. *Journal of Controlled Release,* vol. 99, no. 2004, pp. 241–258.

Edwards, A.; Prausnitz, M. R. (2001): Predicted permeability of the cornea to topical drugs. *Pharmaceutical Research,* vol. 18, pp. 1497–1508.

Edwards, A.; Prausnitz, M. R. (1998): Fiber matrix model of sclera and corneal stroma for drug delivery to the eye. *AICHE Journal,* vol. 44, pp. 214–225.

Schwille, P.; Haupts, U.; Maiti, S.; Webb, W. W. (1999): Molecular dynamics in living cells observed by fluorescence correlation spectroscopy with one- and two-photon excitation. *Biophysical Journal,* vol. 77, pp. 2251–2265.

Masuda, A.; Ushida, K.; Okamoto, T. (2005): New fluorescence correlation spectroscopy enabling direct observation of spatiotemporal dependence of diffusion constants as an evidence of anomalous transport in extracellular matrices. *Biophysical Journal,* vol. 88, pp. 3584–3591.

Boukari, H.; Brichacek, B.; Stratton, P.; Mahoney, S. F.; Lifson, J. D.; Margolis, L.; Nossal, R. (2009): Movements of HIV-Virions in Human Cervical Mucus. *Biomacromolecules,* vol. 10, pp. 2482–2488.

Briandet, R.; Lacroix-Gueu, Renault, M.; Lecart, S.; Meylheuc, T.; Bidnenko, E.; Steenkeste, K.; Bellon-Fontaine, M.-N.; Fontaine-Aupart, M.-P. (2008):

Fluorescence correlation spectroscopy to study diffusion and reaction of bacteriophages inside biofilms. *Applied and Environmental Microbiology,* vol. 74, pp. 2135–2143.

Guiot, E.; Georges, P.; Brun, A.; Fontaine-Aupart, M. P.; Bellon-Fontaine, M. N.; Briandet, R. (2002): Heterogeneity of diffusion inside microbial biofilms determined by fluorescence correlation spectroscopy under two-photon excitation. *Photochemistry and Photobiology,* vol. 75, pp. 570–578.

Gennerich, A.; Schild, D. (2002): Anisotropic diffusion in mitral cell dendrites revealed by fluorescence correlation spectroscopy. *Biophysical Journal,* vol. 83, pp. 510–522.

Loch, C.; Zakelj, S.; Kristl, A.; Nagel, S.; Guthoff, R.; Weitschies, W.; Seidlitz, A (2012): Determination of permeability coefficients of ophthalmic drugs through different layers of porcine, rabbit and bovine eyes. *European Journal of Pharmaceutical Sciences,* vol. 47, pp. 131–138.

Nitsche, J. M.; Chang, H. C.; Weber, P. A.; Nicholson, B. J. (2004): A transient diffusion model yields unitary gap junctional permeabilities from images of cell-to-cell fluorescent dye transfer between Xenopus oocytes. *Biophysical Journal,* vol. 86, pp. 2058–2077.

Petrasek, Z.; Schwille, P. (2008): Precise measurement of diffusion coefficients using scanning fluorescence correlation spectroscopy. *Biophysical Journal,* vol. 94, pp. 1437–1448.

Atkins, P. W. (1994): Physical Chemistry, 5th ed., New York: W. H. Freeman and Company.

Armstrong, J. K.; Wenby, R. B.; Meiselman, H. J.; Fisher, T. C. (2004): The hydrodynamic radii of macromolecules and their effect on red blood cell aggregation. *Biophysical Journal,* vol. 87, pp. 4259–4270.

Braga, J.; Desterro, J. M.; Carmo-Fonseca, M. (2004): Intracellular macromolecular mobility measured by fluorescence recovery after photobleaching with confocal laser scanning microscopes. *Molecular Biology of the Cell,* vol. 15, pp. 4749–4760.

Bu, Z.; Russo, P. S. (1994): Diffusion of dextran in aqueous (hydroxypropyl) cellulose. *Macromolecules,* vol. 27, pp. 1187–1194.

Fahner, E. M.; Grossmann, G. H.; Ebert, K. H. (1984): Elastic and quasielastic light-scattering-studies on the branching characteristics of dextrans. *Die Makromolekulare Chemie,* vol. 185, pp. 2205–2212.

Gregor, T.; Bialek, W.; van Steveninck, R. R. R.; Tank, D. W.; Wieschaus, E. F. (2005): Diffusion and scaling during early embryonic pattern formation. *Proceedings of the National Academy of Sciences of the United States of America,* vol. 102, pp. 18403–18407.

Lawrence, J. R.; Wolfaardt, G. M.; Korber, D. R. (1994): Determination of diffusion-coefficients in biofilms by confocal laser microscopy. *Applied and Environmental Microbiology,* vol. 60, pp. 1166–1173.

Yuan, W.; Lv, Y.; Zeng, M.; Fu, B. M. (2009): Non-invasive measurement of solute permeability in cerebral microvessels of the rat. *Microvascular Research,* vol. 77, pp. 166–173.

Zhang, Z.; Nadezhina, E.; Wilkinson, K. J. (2011): Quantifying diffusion in a biofilm of streptococcus mutans. *Antimicrobial Agents and Chemotherapy,* vol. 55, pp. 1075–1081.

Dix, J. A.; Verkman, A. S. (2008): Crowding effects on diffusion in solutions and cells. *Annual Review of Biophysics,* pp. 247–263.

Lai, S. K.; Wang, Y.-Y.; Hida, K.; Cone, R.; Hanes, J. (2010): Nanoparticles reveal that human cervicovaginal mucus is riddled with pores larger than viruses. *Proceedings of the National Academy of Sciences of the United States of America,* vol. 107, pp. 598–603.

Pels, E.; Beele, H.; Claerhout, I. (2008): Eye bank issues: II. Preservation techniques: warm versus cold storage. *International Ophthalmology,* pp. 155–163.

Sanders, N. N.; De Smedt, S. C.; Demeester, J. (2000): The physical properties of biogels and their permeability for macromolecular drugs and colloidal drug carriers. *Journal of Pharmaceutical Sciences,* vol. 89, pp. 835–849.

Komai, Y.; Ushiki, T. (1991): The three-dimensional organization of collagen fibrils in the human cornea and sclera. *Investigative Opthalmology and Visual Science,* vol. 32, no. 8, pp. 2244–2258.

Sanchez, I.; Martin, R.; Ussa, F.; Fernandez-Bueno, I. (2011): The parameters of the porcine eyeball. *Graefe's Archive for Clinical and Experimental Ophthalmology,* vol. 249, no. 4, pp. 475–482.